



Intense pulsed UV light treatment to design functional optical films from perhydropolysilazane: an alternative to conventional heat treatment processes

Jeong Ju Baek¹, Sung Man Park¹, Yeong Rang Kim¹, Ki Cheol Chang¹, Youn-Jung Heo¹, Geun Yeol Bae¹, Kyung Ho Choi¹, and Gyojic Shin^{1,*} 

¹Green and Sustainable Materials R&D Department, Korea Institute of Industrial Technology, Cheonan-Si 31056, South Korea

Received: 10 June 2021

Accepted: 6 October 2021

Published online:

3 January 2022

© The Author(s), under exclusive licence to Springer Science+Business Media, LLC, part of Springer Nature 2021

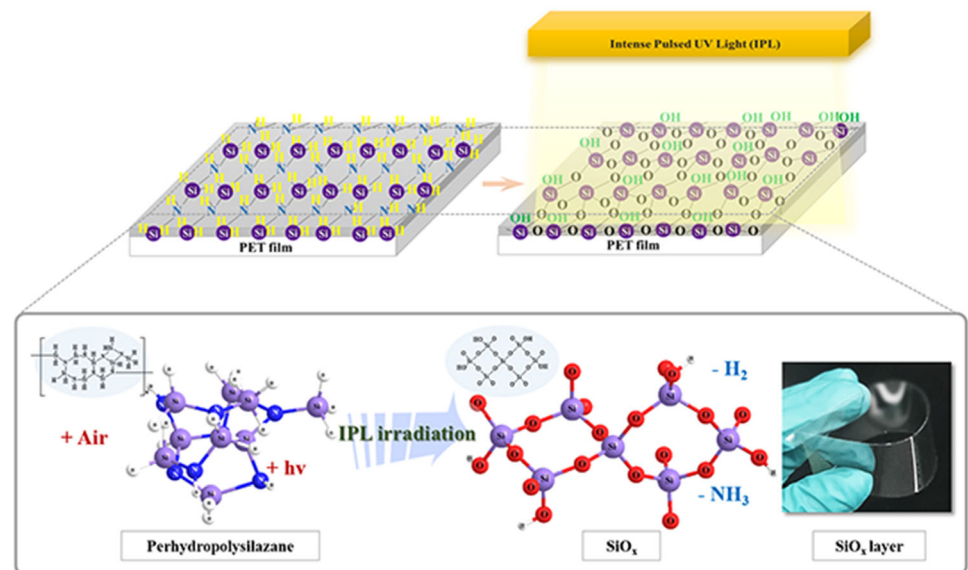
ABSTRACT

Perhydropolysilazane (PHPS) forms a thin layer by solution processing and converts to dense glass-like silica (SiO_x) with excellent chemical resistance, adhesion, and optical properties. However, heat treatment methods for the conversion of PHPS into SiO_x are not sufficient for its application to functional polymer films. In this study, our group developed an alternative process using irradiation by intense pulsed UV light (IPL) at low temperatures in an air environment. We prepared PHPS-derived SiO_x layers using various exposure energies (4.2, 8.4, and 12.6 J cm^{-2}) and then examined their chemical behaviors, compositions, conversion rates, and refractive indices. The resulting SiO_x layer exhibited a 100% conversion rate similar to that of a heat-treated silica layer (600 °C) and a refractive index (RI) value identical to that of amorphous SiO_2 (1.45). Moreover, the final SiO_x thin layer ($160 \text{ nm} \pm 0.7 \text{ nm}$) on a polyethylene terephthalate (PET) film had a transmittance of 90.7% and a pencil hardness of 4H at a load of 750 g. The mean hardness and elastic modulus for the SiO_x layer were 3.25 GPa, and 27.98 GPa, respectively, values similar to those of SiO_x layers formed by roll-to-roll vacuum deposition. Furthermore, the final SiO_x thin layer exhibited no cracks after 100 K bending cycles. Overall, we established that the IPL process is effective for converting PHPS into SiO_x layers on flexible polymer films that have good hardness, elastic modulus, and transparency. It can be applied in large-scale roll-to-roll manufacturing processes to generate functional materials for the optical film industry.

Handling Editor: Maude Jimenez.

Address correspondence to E-mail: gyshin@kitech.re.kr

GRAPHICAL ABSTRACT



Introduction

Silica-based ceramic materials such as silicon nitride (Si₃N₄), silicon oxynitride (SiON), silicon oxycarbonitride (SiCON), and silicon dioxide (SiO₂) exhibit excellent thermal stability and creep, corrosion, and oxidation resistance. As a result, these materials have a variety of applications, such as in insulating [1] and corrosion protection films [2] and as barrier layers [3] in various industries such as electronics, photovoltaics, and automobiles. In general, thick layers of silica-based ceramic materials can be prepared from a diverse array of silica precursors via deposition methods such as physical vapor deposition, chemical vapor deposition, and atomic layer deposition [4–8]. However, these methods require long processing times and high manufacturing costs.

Polysilazane is a versatile silica precursor for generating silica films and has been used for various coating applications in flexible solar cells [9], as gas barrier layers in packaging [10, 11] and electronics [12–14], and as insulating layers in semiconductors [15]. The usefulness of polysilazane in such applications originates from its high hardness, high

transparency, good dielectric properties, and thermal, scratch, and corrosion resistance [16, 17]. In particular, perhydropolysilazane (PHPS) can form dense and glass-like SiO_x with excellent optical properties compared to silica layers derived from other silica precursors, such as tetramethyl orthosilicate or tetraethyl orthosilicate [18–20]. PHPS is also highly soluble in organic solvents and can form thin Si₃N₄- [21] and SiO₂-layered materials that have excellent adhesion to substrates. Thus, polysilazane has attracted significant attention in coating applications across a variety of industries. The unique structure of PHPS, which includes nitrogen atoms that participate in Si–N, Si–H, and N–H bonds, can be converted into SiO_x in the presence of oxygen and moisture, depending on the annealing atmosphere [22].

Numerous studies have investigated the conversion of PHPS to SiO₂ using vacuum deep ultraviolet (VUV) ($\lambda = 172\text{--}222\text{ nm}$) treatment [23–30], ammonium hydroxide or hydrogen peroxide solutions, various catalysts, and thermal treatments, among other methods [31–34]. However, thermal treatments and processes that use ammonium hydroxide and hydrogen peroxide vapor are not suitable for

generating functional polymer films because of the chemical instability of the polymer substrate, long processing times, and the use of high temperatures. Moreover, VUV processes require more than one hour to achieve the necessary conversion, and simultaneous control of the oxygen concentration and temperature of the coatings to generate dense silica layers is required [23]. In addition, the VUV process is not suitable for the treatment of aromatic polymer films because these polymers are vulnerable to UV irradiation. Thus, more efficient conversion processes are required to commercialize PHPS-derived functional polymer films. Polymer films, especially polyethylene terephthalate (PET) films, have been used in a wide range of applications, including in the packaging industry, flexible displays, and touch panels, because of their high transparency and chemical stability, but they also have drawbacks, such as low scratch resistance and gas permeability.

Intense pulsed UV light (IPL) processes have been applied in semiconductor manufacturing processes for heat treatment and sterilization to clean the surfaces of glass and Si wafers. Moreover, IPL methods have been exploited for sintering inorganic materials and curing organic materials in the roll-to-roll processing of electronic inks and in the solar cell industry [35–38]. The advantages of the IPL process include its applicability to large areas and its ability to irradiate at high energies for short time periods at low temperatures in an air environment without requiring additional heat treatment, gas control, or the generation of ozone, which are necessary for VUV.

In a previous study [39], our group reported on the efficiency of PHPS-derived SiO₂ gate dielectric layers fabricated using IPL on silicon wafers. Thus, in this study, we propose an IPL process applicable to polymer substrates that can be performed more rapidly and at lower temperatures than VUV methods. Systematic studies of PHPS-derived SiO₂ layers induced by IPL are uncommon and do not provide a sufficient understanding of the processing method and the resulting materials. Thus, it is important to conduct detailed studies to examine the influence of irradiation conditions on the chemical composition and surface properties of these important SiO₂ layers.

In this study, we investigated the conversion of PHPS into a silica layer by IPL irradiation and compared it to materials prepared using conventional heat treatment and VUV processes [23, 25, 27].

Moreover, we evaluated the conversion behavior of PHPS and the properties of the resulting thin silica layers on PET substrates. Because the IPL process is conducted at low temperatures in an air environment, these results are important for advancing these materials for large-scale roll-to-roll manufacturing processes.

Experimental details

Materials

PHPS [$M_n = 1500\text{--}1700$ g/mol, $M_w = 14,000\text{--}15,000$ g/mol, PDI = 2.3–2.5, 18 wt.% in dibutyl ether (DBE); DNF Co., Korea] without a catalyst was used as the precursor material. Non-alkaline glass (thickness 500 μm , code number: C5B0D0Z10, Corning Inc., USA), silicon (Si) wafers (thickness 525 ± 25 μm , Silicon Technology Co. Ltd., Japan), KBr windows (thickness 4000 μm , Thermo Scientific Inc., USA), PET films (thickness 150 μm , SK Chemical Co. Ltd., Korea), and colorless polyimide (CPI) films (thickness 50 μm , Kolon Industries Inc., Korea) were used as substrates for the PHPS coating.

Preparation of silica layers

The glass and Si wafer substrates were processed into 40 mm \times 40 mm pieces and then sequentially cleaned in an alkali solution, acetone, and isopropyl alcohol. The samples were subsequently dried in a convection oven for 1 h. Then, a 5 wt.% PHPS solution in DBE, which was prepared by diluting an 18 wt.% PHPS solution into DBE, was coated onto the substrates using a spin coater at 1000 rpm for 10 s. Various substrates were used to prepare samples for different analyses: a KBr window was used for Fourier-transform infrared spectroscopy (FT-IR) measurements, a non-alkaline glass substrate was used for X-ray photoelectron spectroscopy (XPS) analyses and contact angle measurements, and a Si wafer was used for ellipsometry measurements. After coating, the PHPS layer on each substrate was pre-baked at 120 $^\circ\text{C}$ for 1 min on a hotplate. The resulting PHPS layers were converted into silica layers by IPL irradiation using a mounted xenon lamp (width \times length, 25 mm \times 400 mm) at a power of 750 W, an applied voltage of 3000 V, a pulse width of 100 μs , and a frequency of 12.4 Hz. Total energies of 4.2, 8.4,

and 12.6 J cm^{-2} were applied by using 1000, 2000, and 3000 intense UV pulses, respectively. The linear spot size of irradiation was 50 mm wide and 400 mm long at a distance of 50 mm. This process resulted in hydrolysis and polycondensation reactions in the PHPS layers. Finally, we observed the structural transformation and surface properties of the silica layer using FT-IR spectroscopy, ellipsometry, contact angle measurements, and XPS.

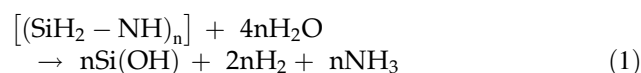
We also prepared control silica layers by heat treating PHPS-coated samples at 250, 350, 450, and 600 °C for 1 h in an air environment in a tube furnace. These control samples served as a comparison for the SiO_x layers prepared using the IPL process. Additional samples were prepared by coating 3, 5, and 10 wt.% PHPS solutions in DBE onto Si wafers using a spin coater at 1000 rpm for 10 s and then prebaking the samples at 120 °C for 1 min in air on a hotplate. This series of samples was used to examine variations in the thickness and RI of PHPS-derived SiO_x layers prepared using IPL (total energy of 12.6 J cm^{-2}) and heat treatment (600 °C, 1 h) using ellipsometry and field-emission scanning electron microscopy (FE-SEM) measurements.

Finally, the optical properties of the PHPS-derived- SiO_x layers prepared using IPL were evaluated to establish the applicability of such materials as functional optical coatings (which require transparent and hard films). PHPS was coated onto PET films (40 mm × 40 mm) using 3 wt.% and 5 wt.% PHPS solutions in DBE by using a spin coater at 1000 rpm for 10 s. Then, the PHPS layers were prebaked at 120 °C for 1 min in air on a hotplate. Additionally, bending test samples coated with 5 wt.% PHPS on PET films (50 mm × 100 mm) and 5 wt.% PHPS on colorless polyimide (CPI) films (50 mm × 100 mm) were prepared in the same manner as previously described. These PHPS layers were converted into silica layers by IPL irradiation using an applied voltage of 3000 V, a pulse width of 100 μs, 3000 UV pulses, and a frequency of 12.4 Hz (total energy of 12.6 J cm^{-2}). The pencil hardness, transmittance, roughness, adhesion, mechanical properties, and crack tendency were then examined, as described in “[Instruments and characterization](#)” section.

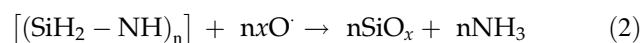
PHPS conversion studies

Two different mechanisms have been proposed for the conversion of PHPS into SiO_x [24]. First, in the

presence of water, an oxidative process occurs that specifically involves the hydrolysis of both the Si–N and Si–H bonds, which results in the release of ammonia and hydrogen and the formation of silanol groups. The reaction for this process is shown in Eq. (1) [40].



The intermediate silanol groups react and transform into a SiO_x network in a manner similar to standard sol–gel processes. This mechanism occurs under heat treatment in the presence of moisture, using either ammonium hydroxide or hydrogen peroxide as a catalyst. The second mechanism, which was proposed by Naganuma et al., involves high-energy photons generated by VUV irradiation, which causes the dissociation of chemical bonds and the generation of ozone molecules (O_3) and oxygen radicals $\text{O} (1\text{D})$. This results in the direct substitution of an Si atom with activated oxygen and ultimately the formation of a SiO_x network [Eq. (2)].



Several reports demonstrate that this method of irradiation with VUV light minimizes shrinkage of the film and thus prevents cracking of the layer material [27].

Instruments and characterization

An IPL system (X-1100, Xenon Co.) was used to convert PHPS into silica layers. The exposure energy in the UVC range ($\lambda = 250\text{--}260 \text{ nm}$) was measured using a photometer (UV PowerPuck 2, EIT Instrument Markets). Chemical changes in the PHPS were investigated using FT-IR (Nicolet 6700, Thermo Fisher Scientific). The surface morphology and thickness of the samples were investigated using FE-SEM (JEOL JSM-7500F) at 10 kV. In these electron microscopy analyses, the measurement samples were coated with platinum to prevent charging during observation. Focused ion beam milling was used to prepare cross-sectional samples to visualize the interface between the PHPS coating and the PET film. The surface and internal chemical compositions of the coating layers were evaluated using an XPS system (K-Alpha, Thermo Fisher Scientific) with an Al $K\alpha$ (1486.6 eV) source, which was calibrated using the C1s binding energy at 284 eV. XPS depth profile measurements were performed by

sputtering the samples with Ar^+ ions at 3 kV. The surface properties of PHPS were determined using a pencil hardness tester (LT-PC2, Lab & Tools) and a contact angle measurement system (Phoenix 150, S.E.O. Co., Ltd.). For the hardness test, a pencil was moved over the surface at a 45° angle with a load of 750 g. The contact angle was measured with a 10- μL water droplet by the tangent line method using a camera (zoom lens $\times 12$) with a white LED light source. The surface roughness of the final layer was evaluated using atomic force microscopy (AFM; XE-100, Park Systems) in contact mode. The transmittance of the film was measured using a UV spectrophotometer (UV-3600, Shimadzu). The RI and thickness as a function of wavelength (240–1040 nm) were measured using an ellipsometer (SEN Research 4.0, SENTECH). The SiO_x film was prepared on a Si wafer with an angle of incidence of 70° . After measuring five different locations, the RI was obtained by applying the Cauchy transparent model. The adhesion properties of the silica layers coated onto PET substrates were examined using a cross-cut tape tester (YCC-230/1, Yoshimitsu, Japan). A grid (10 \times 10 sections) with meshes 1 mm \times 1 mm in size was made using a cross-cut guide and a utility knife. Pressure-sensitive adhesive tape (CT-15, Nichiban Co., Ltd., Tokyo, Japan) was attached to the grid and rubbed by a finger to adhere the tape completely to the film. The tape was then sharply removed vertically from the surface. The grid was then observed using an optical microscope (OM) (BX51, Olympus, Japan) and a three-dimensional (3D) laser scanning confocal microscope (VK-1000, KEYENCE Co., USA). The nano-mechanical properties of the films were examined using a nano-indenter (TI950, Hysitron Inc., USA). Indentations were made using a three-sided pyramid Berkovich indenter with a load of 20 μN , a loading time segment of 5 s, a load-holding time of 2 s, and an unloading time of 5 s. The hardness and elastic modulus were calculated from the unloading regions of the load-displacement (P-h) curves using the Oliver and Pharr method. Dynamic bending tests of the films were performed using a tension-free U-shaped folding test machine (DLDMLH-FS/FU, YUASA).

Results and discussion

Chemical behavior of PHPS-derived SiO_x materials

The radiation source for the IPL method was generated by an arc plasma phenomenon via a xenon flash

lamp. This source provides stronger energy over short time periods than ordinary UV lamps. Thus, IPL from a xenon lamp (which produces radiation with wavelengths of 100–1100 nm) quickly penetrates the PHPS layer to provide excellent curing without heat damage or thermal shrinkage to the substrates, including polymers. Only a small amount of heat is imparted to the material when high-energy radiation is applied over very short pulse durations and large processing areas. Moreover, irradiation can be implemented with photon energies ranging from 4.43–12.4 eV with associated wavelengths of 100–280 nm, which correspond to ultraviolet B and C (UVB, UVC) in the electromagnetic spectrum. This energy source is sufficient to dissociate Si–N and Si–H bonds, permitting these elements to react with oxygen atoms. Radiation by this IPL method penetrates materials more deeply than VUV because of the different wavelength ranges for these two sources. Thus, IPL processes are thought to be more suitable for preparing functional optical films.

Samples using 5 wt.% PHPS solutions and irradiated at different exposure energies and heat treatments were investigated using FT-IR spectroscopy. Importantly, all materials used in these FT-IR studies were prepared on KBr substrates. Specifically, the conversion rates were calculated by comparing the intensities of the absorption peaks in the irradiated material samples with those of a reference sample that was cured by heat treatment at 600 $^\circ\text{C}$ for 1 h. Thermal gravimetric analysis (TGA) analyses revealed that, at temperatures above 400 $^\circ\text{C}$, most of the N–H and Si–H moieties in PHPS converted to hydroxyl groups. At temperatures above 600 $^\circ\text{C}$, the Si–OH groups subsequently converted to SiO_x [41, 42]. Importantly, the reference sample was prepared at 600 $^\circ\text{C}$ because of the low melting point (734 $^\circ\text{C}$) of KBr substrates. The exposure energies were 4.2 J cm^{-2} (1000 pulses), 8.4 J cm^{-2} (2000 pulses), and 12.6 J cm^{-2} (3000 pulses), as measured using a photometer. The process time was less than 10 min, and the surface temperature of the silica was below 65 $^\circ\text{C}$ after IPL irradiation.

The FT-IR spectra acquired from the materials after IPL irradiation are shown in Fig. 1a, and the corresponding peak assignments are listed in Table 1 [41, 43]. Increasing the intensity of the IPL irradiation dose (4.2, 8.4, and 12.6 J cm^{-2}) caused the intensities of absorption peaks assigned to N–H stretching (3370 cm^{-1}), Si–H stretching (2160 cm^{-1}), and Si–N–

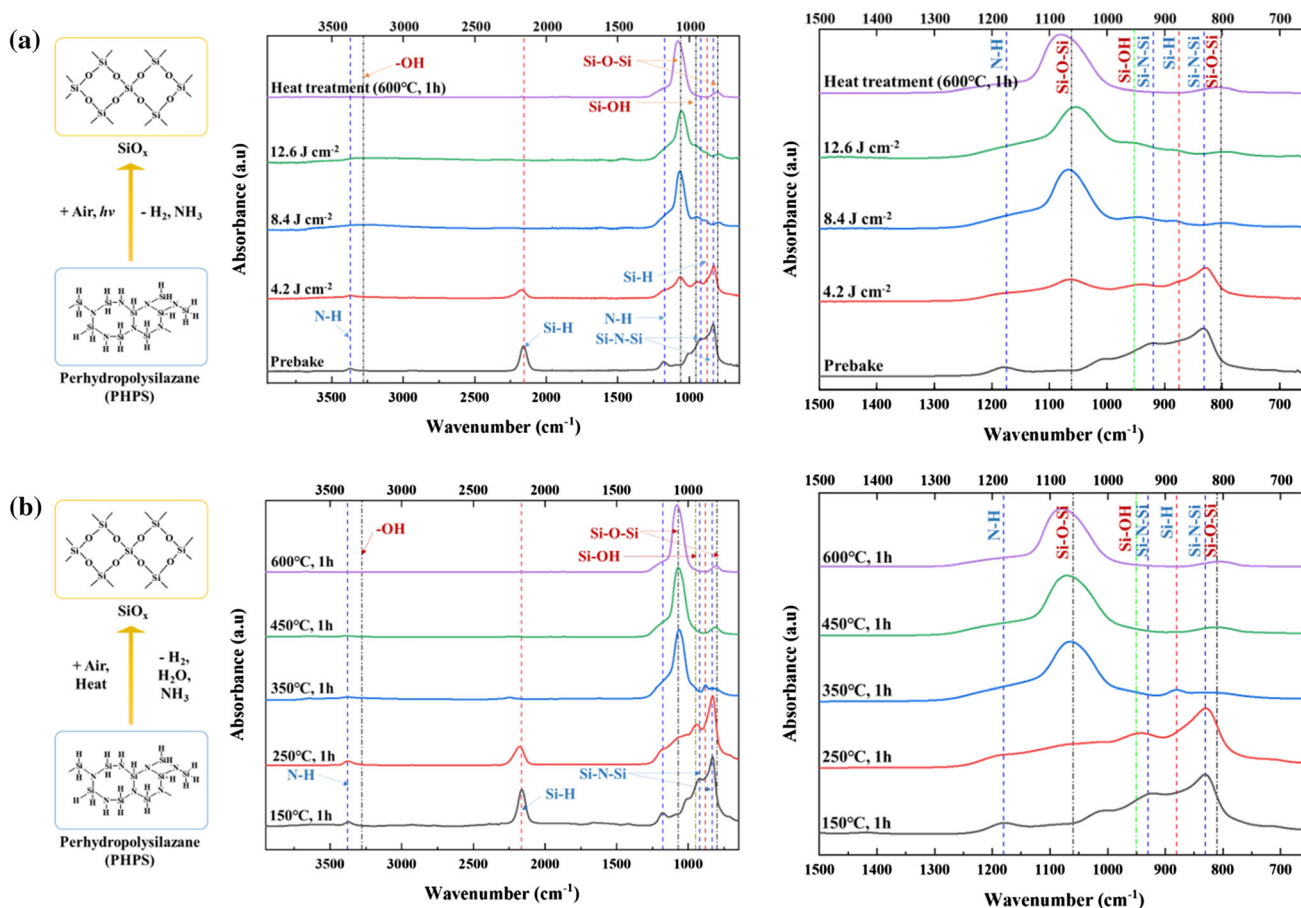


Figure 1 FT-IR spectra of 5 wt.% PHPS-derived layer materials acquired at different steps in the process, specifically after the prebake step: **a** after application of IPL with different exposure

energies and **b** after heat treatment at temperatures of 250, 350, 450, 600 °C for 1 h in a furnace.

Table 1 Assignments for FT-IR absorption bands for the various products of PHPS

Wavenumber (cm ⁻¹)	Assignment	Wavenumber (cm ⁻¹)	Assignment
3370	N–H, stretching	1180	N–H, bending
2160	Si–H, stretching	880	Si–H, wagging
920, 840	Si–N–Si, stretching	950	Si–OH, stretching
1080	Si–O–Si, asymmetrical	800	Si–O–Si, symmetrical

Si stretching (920, 840 cm⁻¹) to decrease. Concomitantly, the intensity of the Si–O–Si stretching peak (1080 cm⁻¹, 800 cm⁻¹) increased. The broad O–H stretching peak at approximately 3450–3000 cm⁻¹ indicates the formation of silanol groups during the IPL process. Moreover, Si–N–Si (920 and 840 cm⁻¹) and Si–OH (950 cm⁻¹) stretching peaks were also observed. These results establish that the Si–N and Si–H bonds dissociated during the IPL process, which was accompanied by the incorporation of oxygen into the materials via oxygen radicals from the atmosphere. These results are similar to those

observed for PHPS conversion via VUV processes [25, 27]. However, while Si–H and Si–N bonds were dissociated by IPL irradiation, activated oxygen species such as excited singlet oxygen [O(1D)] and hydroxyl radicals (OH*) derived from O₂ and H₂O in air atmosphere were generated simultaneously during IPL irradiation [44]. The Si atoms were directly substituted with activated oxygen and hydroxyl radicals; afterward, most of Si atoms formed SiO_x and some of hydroxyl groups associated with Si atoms were oriented at the surface based on the water contact angle and XPS results (as discussed below).

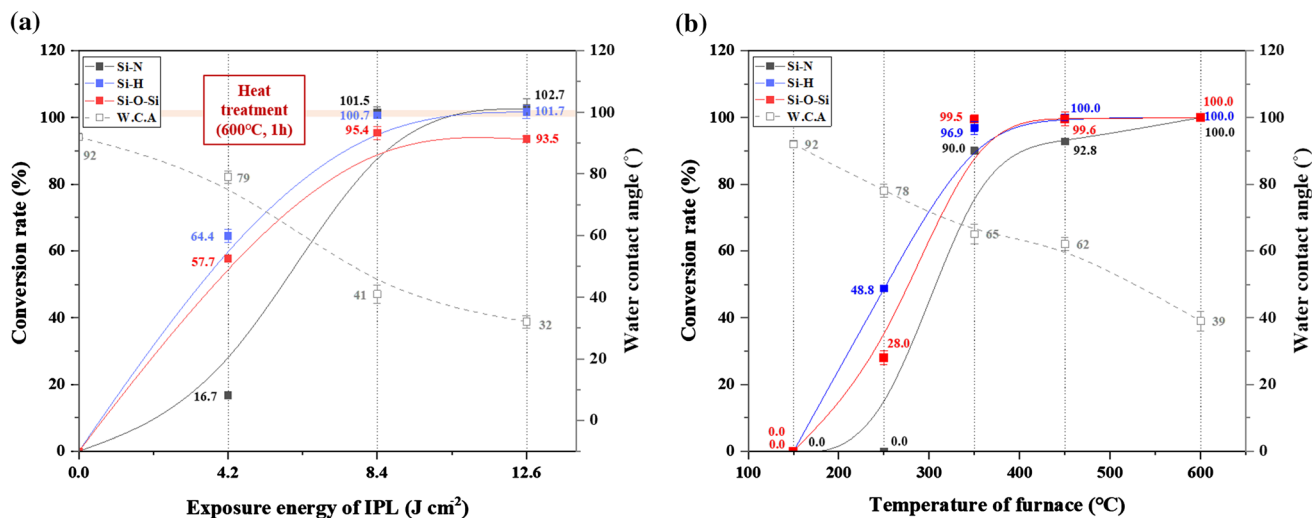


Figure 2 Conversion rate and WCA of 5 wt.% PHPS layers subjected to **a** IPL treatment as a function of exposure energy and **b** heat treatment as a function of temperature.

The FT-IR spectra of the materials after heat treatment are shown in Fig. 1b. Increasing the heat treatment temperature (250, 350, 450, and 600 °C) caused the absorption peaks arising from N–H stretching (3370 cm⁻¹), Si–H stretching (2160 cm⁻¹), and Si–N–Si stretching (920 and 840 cm⁻¹) to decrease in intensity. In comparison, the intensity of the Si–O–Si stretching peaks (1080 cm⁻¹ and 800 cm⁻¹) increased in intensity. Interestingly, the broad O–H stretching peak at 3450–3000 cm⁻¹ was not observed, which is in contrast to materials prepared using IPL irradiation. These results indicate that the intermediate silanol groups were completely transformed into a SiO_x network.

Conversion rate of PHPS-derived SiO_x materials

The effects of IPL irradiation on the conversion rate were quantified by comparing the FT-IR absorption peak intensities of layers prepared under the same coating conditions (thickness 160 nm, STD = 0.7 nm) but subjected to different heat treatments. The intensity changes of the peaks related to SiO_x formation after heat treatment (600 °C for the reference sample)—the Si–N–Si stretching peak (840 cm⁻¹), Si–O–Si asymmetric stretching peak (1080 cm⁻¹), and Si–H stretching peak (2160 cm⁻¹)—were considered to correspond to 100% conversion. [The integral area of the peaks was difficult to calculate because the Si–N peak (840 cm⁻¹) overlapped with other peaks.]

Changes in the intensities of these selected peaks (840 cm⁻¹, 1080 cm⁻¹, and 2160 cm⁻¹) for the samples prepared by IPL treatment and the heat-treated references were compared according to Eq. (3).

$$\text{Conversion rate (\%)} = (I_{\text{UVC}} - I_{\text{PB}}) / (I_{\text{HT}} - I_{\text{PB}}) \times 100 \quad (3)$$

where I_{UVC} is the intensity of the sample cured by IPL irradiation or heat treatment, I_{HT} is the intensity of the reference sample cured in a furnace at 600 °C, and I_{PB} is the intensity of prebaked PHPS on a KBr substrate.

As shown in Fig. 2a, the conversion rates calculated from the Si–N–Si, Si–O–Si, and Si–H stretching peaks were 16.7%, 57.7%, and 64.4%, respectively, at the lowest IPL energy of 4.2 J cm⁻². The relatively high conversion rate of the Si–H moieties versus the Si–N stretching peaks after only 4.2 J cm⁻² of energy is thought to arise from the strong Coulombic attractions among the negatively charged nitrogen species and positively charged silica species of Si–N. The Si–H bonds dissociated more readily than the Si–N bonds owing to their relatively lower binding energy (3.7 eV for Si–H and 4.9 eV for Si–N), which contributed to the formation of Si–O bonds as Si combined with the activated oxygen that formed during IPL irradiation. After exposure to IPL energies of 8.4 J cm⁻², the conversion rates measured via the Si–N and Si–H stretching peaks were above 100% with respect to the reference sample, but the conversion rate as determined by the Si–O–Si stretching

peak was 95.4%. At IPL energies of 12.6 J cm^{-2} , the conversion rates determined from both the Si–N and Si–H stretching peaks increased but that determined from the Si–O–Si stretching peak decreased to 93.5%. This means that IPL energies above 8.4 J cm^{-2} did not promote increased SiO_x network formation. At such higher energies, silanol groups preferably formed, as revealed by the FT-IR and XPS analyses (as discussed below).

As shown in Fig. 2b, at $250 \text{ }^\circ\text{C}$, the conversion rates calculated from the Si–N, Si–O–Si, and Si–H stretching peaks were 0%, 28.0%, and 48.8%, respectively. The conversion rates calculated from the Si–N, Si–O–Si, and Si–H stretching peaks increased rapidly as the temperature increased to $350 \text{ }^\circ\text{C}$ and attained 100% conversion at a temperature of $600 \text{ }^\circ\text{C}$.

Naganuma et al. reported the formation of a silica layer by using VUV irradiation at a wavelength of 172 nm for 1 h in dry air at a relative humidity of less than 2% [27]. Moreover, Ohishi and Yamazaki reported that VUV irradiation for 2 min without heat treatment did not yield a fully formed silica layer. [25] The above results demonstrate that the conversion of PHPS to SiO_x using IPL is more rapid than that using VUV irradiation and does not require additional heat treatment or precise temperature control. However, the residual hydroxyl groups in the SiO_x layer materials derived by IPL irradiation, which were much fewer for the materials prepared by heat treatment, influenced the surface hydrophilicity of SiO_x layers, as shown in Fig. 2a and b. In other words, the water contact angles of the SiO_x layers derived by IPL irradiation were lower than those prepared by heat treatment.

Thickness and refractive index of SiO_x layer from ellipsometry measurements

Spectroscopic ellipsometry is a routine and powerful analytical technique for measuring the film thickness and RI of single layers and multilayer stacks of materials.

The thicknesses of the SiO_x layers prepared on Si wafers from 3, 5, and 10 wt.% PHPS solutions using IPL irradiation (12.6 J cm^{-2}) and heat treatment ($600 \text{ }^\circ\text{C}$, 1 h) are shown in Fig. 3. The thicknesses of the silica layers produced using IPL irradiation were approximately $93 \pm 1.7 \text{ nm}$, $160 \pm 0.7 \text{ nm}$, and $364 \pm 0.5 \text{ nm}$ for the 3, 5, and 10 wt.% PHPS solutions, respectively. The thicknesses of the silica layers

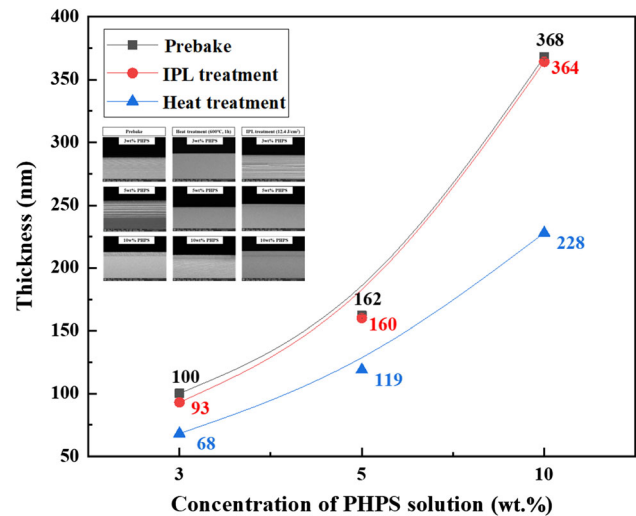


Figure 3 Thickness variation of 3 wt.%, 5 wt.%, and 10 wt.% PHPS on Si wafers subjected to IPL treatment (12.6 J cm^{-2}) and heat treatment ($600 \text{ }^\circ\text{C}$, 1 h) in a furnace obtained via ellipsometry.

produced by using the heat treatment were approximately $68 \pm 1.5 \text{ nm}$, $119 \pm 1.2 \text{ nm}$, and $228 \pm 0.8 \text{ nm}$ for the 3, 5, and 10 wt.% PHPS solutions, respectively. Thus, the thickness variation of the SiO_x layer derived by heat treatment was larger than that derived by IPL irradiation, which showed a thickness similar to the initial value. Additionally, the thickness values measured using ellipsometry were similar to those measured using FE-SEM. These results indicate that either a decrease in porosity or an increase in the atomic packing density does not occur during IPL irradiation. Thus, we posit that the shrinkage rate of PHPS-derived SiO_x layers upon IPL irradiation would be low, thus minimizing deformation of the polymer films.

The RI values of SiO_x prepared on Si wafers using the 5 wt.% PHPS solution and IPL irradiation at 4.2, 8.4, and 12.6 J cm^{-2} and heat treatment at 150, 250, 350, 450, and $600 \text{ }^\circ\text{C}$ are shown in Fig. 4. Increasing the intensity of IPL irradiation caused the RI of the PHPS layer to decrease from 1.55 to 1.45, which is similar to the RI of amorphous SiO_2 (1.45). Increasing the temperature of the heat-treated samples also caused the RI value of the PHPS layer to decrease from 1.55 to 1.45. The RI value of the PHPS-derived SiO_x layer material derived by IPL irradiation at an energy of 4.2 J cm^{-2} was measured to be 1.49, which compares well with that derived by heat treatment at 250– $350 \text{ }^\circ\text{C}$. The RI value of the PHPS-derived SiO_x layer derived by IPL irradiation at an energy of

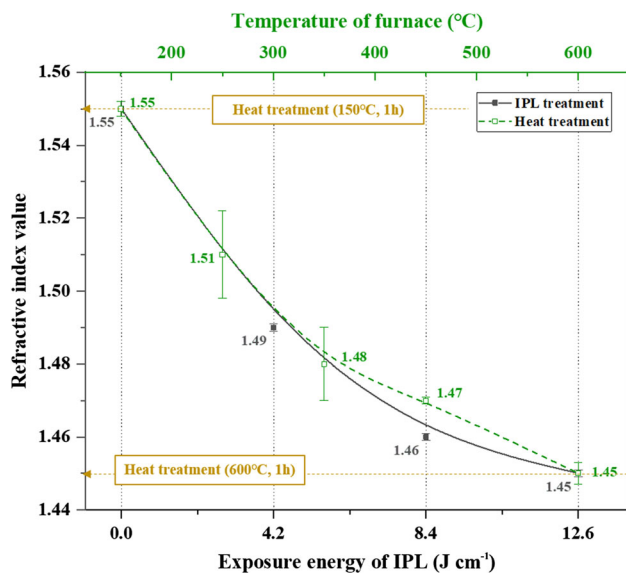


Figure 4 RI value of a 5 wt.% PHPS layer subjected to IPL treatment as a function of exposure energy (4.2, 8.4, and 12.6 J cm⁻²) and heat treatment as a function of temperature (150, 250, 350, 450, and 600 °C).

8.4 J cm⁻² was 1.46, which agrees well with that derived from heat treatment at 450 °C. The RI value of the PHPS-derived SiO_x layers prepared using IPL irradiation at an energy of 12.6 J cm⁻² was 1.45, which was the same as that derived from heat treatment at 600 °C. Higher RI values correspond to higher nitrogen contents because of the relatively lower polarizability of Si–O bonds versus Si–N bonds [45].

Thus, we established that IPL-irradiated PHPS layers were converted into SiO_x under an air atmosphere, without needing to control the oxygen concentration or apply additional heat treatment.

Chemical composition of SiO_x layer from XPS analysis

The XPS survey scans acquired from the 5 wt.% PHPS film before and after IPL irradiation are shown in Table 2, which focuses on three key elements: Si, N, and O. As shown in Table 2, the O1s content increased with increasing applied energy, whereas the N1s content decreased with increasing energy, as predicted. Moreover, we established that a small amount of nitrogen remained after the film was converted to a silica layer. The average composition of the layer was SiO_{1.47}N_{0.10}, which was attributed to the fact that the top surface of the SiO_x layer formed first, which gradually prevented the diffusion of oxygen, as reported previously [42]. This is confirmed in Fig. 5b, which shows the depth profile of the 5 wt.% PHPS material prepared with IPL treatment at 8.4 J cm⁻².

The narrow XPS scans in Fig. 6a–c reveal that the binding energies of prebaked PHPS (i.e., prior to IPL treatment) were 101.2 eV (Si2p), 531.9 eV (O1s), and 397.9 eV (N1s). These peaks shifted to 103.0 eV (Si2p), 532.2 eV (O1s), and 398.4 eV (N1s) after IPL irradiation. The O1s peak increased and the N1s peak decreased in intensity with increasing exposure energy, which is in agreement with the FT-IR results. The XPS results also provide evidence for the conversion of the PHPS layer to a SiO_x layer by IPL irradiation. The binding energy of SiO₂ was established to be 103.6 eV for the Si2p in a previous study [42]. However, the binding energy of Si2p for the SiO_x layer materials prepared using heat treatment was closer to 103.6 eV than that for the materials prepared

Table 2 XPS survey results for 5 wt.% PHPS-derived layers (non-etched) prepared by using IPL. (a) Relative elemental fraction (at.%) and (b) atomic ratios of the coatings with respect to Si after processing via IPL or heat treatment

Process conditions	Intense pulsed UV light (IPL)				Heat treatment	
	Number of pulses	Exposure energy (J cm ⁻²)	Duration time (s)	Substrate temp. (°C)		
	0	4.2	8.4	12.6	600 °C for 1 h	
	0	80.1	160.2	240.3		
	24.0	46.2	57.8	61.2		
(a) At.%	Si 2p	51.39	57.81	39.03	38.40	39.12
	O 1s	16.99	21.27	55.16	56.44	57.49
	N 1s	31.63	20.47	4.65	3.87	2.63
(b) Atomic ratio	O/Si	0.33	0.37	1.41	1.47	1.47
	N/Si	0.62	0.35	0.12	0.10	0.07

using IPL irradiation owing to the presence of silanol groups in the SiO_x layer after IPL irradiation, as revealed by deconvoluting the Si2p and O1s narrow XPS spectra in Fig. 7. Both Si–N bonds and Si–OH bonds were present after IPL treatment at 12.6 J cm⁻², whereas these bonds were not present or were present only in small quantities in the heat-treated samples prepared at 600 °C for 1 h. These results were also corroborated by the FT-IR results.

XPS depth profiles conducted at identical etching energies permit the prediction of the thickness, hardness, and composition in thin layers. As shown in the XPS depth profiles of the 5 wt.% PHPS materials prepared with IPL treatment (Fig. 5a–c), the

irradiation dose influenced the atomic composition of the cured layer. In particular, longer irradiation times resulted in the formation of a uniform and dense thin silica layer owing to an increase in the degree and depth of curing. Longer etching times were required for samples prepared with a higher number of irradiation doses. Moreover, we propose that the composition of the layers varied in the depth direction of the film, depending on the exposure energy (which determines the penetration depth of the IPL).

As shown in the XPS depth profiles of the 5 wt.% PHPS-derived SiO_x layer materials prepared by heat treatment at 600 °C for 1 h (Fig. 5d), it took less time to etch the SiO_x layer than the cured layer, which was

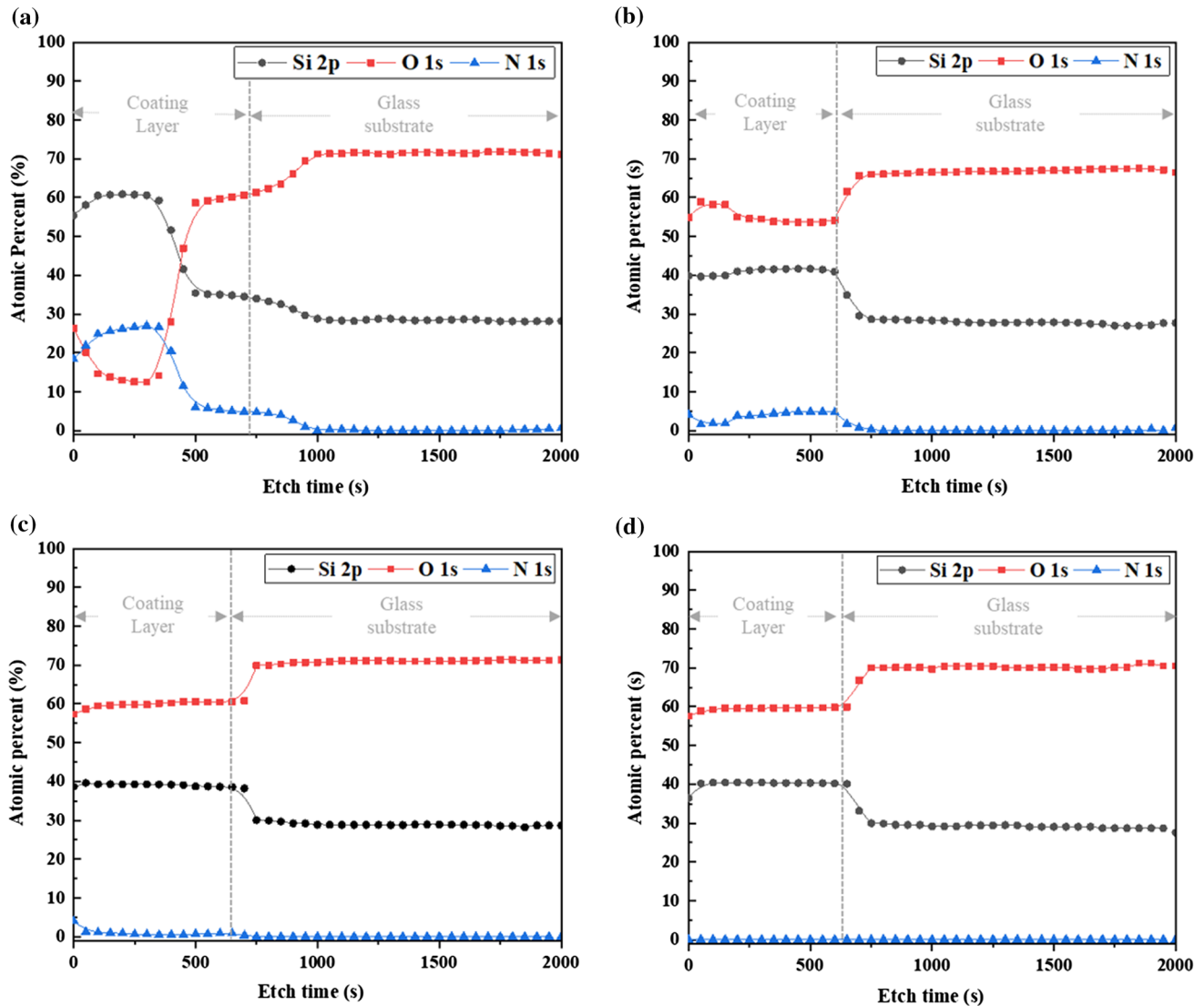


Figure 5 XPS elemental depth profiles of 5 wt.% PHPS layers prepared using IPL pulses with total energies of **a** 4.2, **b** 8.4, and **c** 12.6 J cm⁻² and **d** heat treatment at a temperature of 600 °C for 1 h in a furnace.

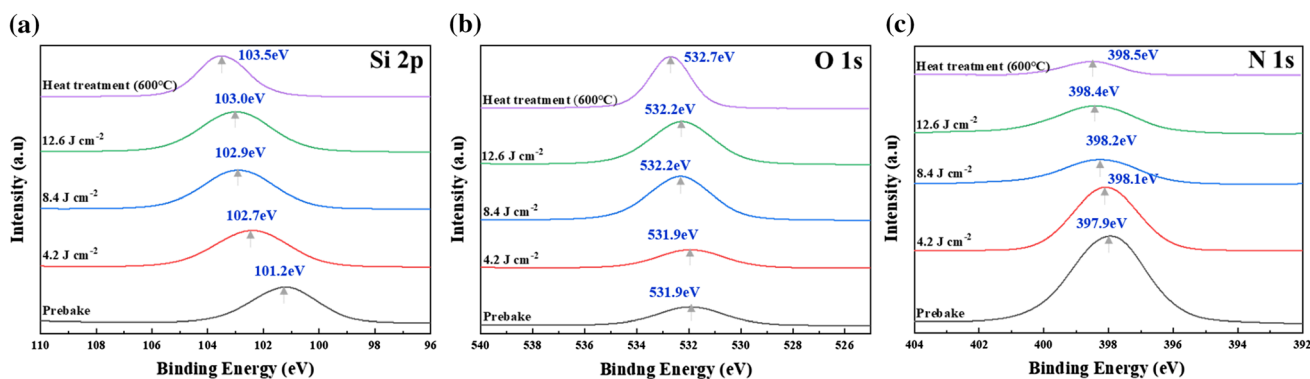


Figure 6 XPS binding energy spectra for **a** Si 2p, **b** O 1s, and **c** N 1s of a 5 wt.% PHPS layers prepared using IPL irradiation using various applied energies (4.2, 8.4, and 12.6 J cm⁻²) and heat treatment (600 °C, 1 h).

attributed to the thinner silica layer and increased binding energy of Si2p.

We predicted that for thinner films than those studied here (i.e., thickness 160 nm, STD = 0.7 nm), higher conversion rates of PHPS into silica could be achieved. Such results are supported by samples prepared by VUV irradiation reported by Naganuma et al. [27].

Chemical composition as a function of PHPS film thickness

Based on the above IR and XPS analyses, we explored enhancing the conversion rate of the PHPS layers by preparing materials with different thicknesses. This was achieved by coating 3 wt.% PHPS diluted in DBE onto glass substrates by using coating conditions of 1000 rpm and irradiation via IPL with a dose of 12.6 J cm⁻². This resulted in a film thickness of 93 nm (STD = 1.7 nm). Then, the composition of the cured layers was examined using XPS. As shown in Table 3, the ratios of O/Si and N/Si species depended on the PHPS concentration and thus the film thickness. The 3 and 5 wt.% PHPS-derived SiO_x layers via IPL irradiation had O/Si ratios of 1.84 and 1.47, respectively, which were greater than and equal to, respectively, the O/Si ratio for the SiO_x layer materials derived using heat treatment (1.47). Moreover, the O/Si ratios were closer to those of amorphous SiO₂, whereas the N/Si ratios (0.06) of the cured layer were lower for thinner films. These changes in the atomic ratios are thought to arise from the increased conversion rates owing to the decreased coating thickness. The coating layers produced by the 3 and 5 wt.% PHPS solutions yielded layers with compositions of SiO_{1.84}N_{0.06} and SiO_{1.47}N_{0.10}, respectively.

These values are similar to those of films derived by VUV (O/Si ratio for 5 wt.% PHPS was 1.5–1.6), as reported previously [27]. Thus, the IPL process can effectively form SiO_x layers more rapidly than VUV and heat treatment processes without the need for additional heat treatment. Furthermore, these data show that silica layers of different compositions can be formed with PHPS by controlling the coating thickness.

The XPS depth profiles in Fig. 8 show that dense silica layers of different thicknesses formed after IPL irradiation at a coating thickness of 93 nm (3 wt.% PHPS, STD = 1.7 nm) and 160 nm (5 wt.% PHPS, STD = 0.7 nm) at an irradiation energy of 12.6 J cm⁻².

Surface properties of SiO_x layers on PET film

PHPS films with different thicknesses were coated onto PET film substrates using the same coating conditions (1000 rpm), 3 or 5 wt.% PHPS diluted in DBE, and an IPL irradiation dose of 12.6 J cm⁻². The water contact angles (WCAs) of the layers were measured to evaluate hydrophilicity of the film. The WCAs of the prebaked samples prepared with 3 and 5 wt.% PHPS solutions were both 92 ± 1° (Fig. 2); after IPL treatment, the WCAs decreased to 23 ± 2° and 32 ± 2°, respectively, as shown in Table 4. The decrease in WCA with decreasing PHPS concentration after IPL treatment is attributed to a decrease in surface roughness. Thus, the surface changed from hydrophobic (the WCA of PET is 74 ± 2°) to hydrophilic owing to the IPL treatment as a result of the increase in surface energy, which corresponds to the

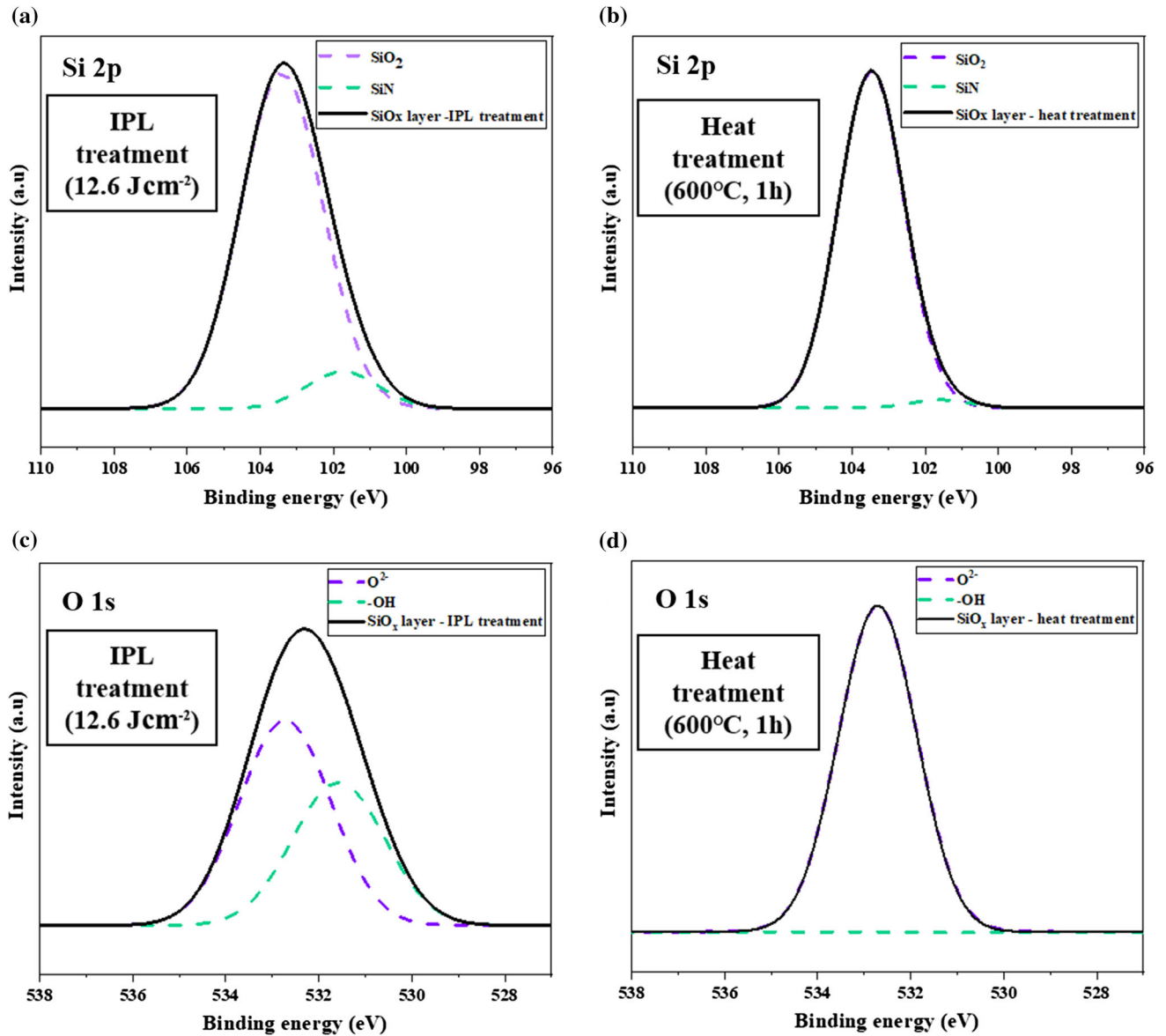


Figure 7 Deconvoluted Si 2p, O1s XPS narrow spectra of **a, c** 5 wt.% PHPS films prepared using IPL irradiation (12.6 J cm^{-2}), and **b, d** heat treatment (600°C , 1 h).

Table 3 XPS survey results of PHPS-derived SiO_x layers of various thicknesses prepared using IPL irradiation. (a) Atomic % of the elements of interest and (b) atomic ratios with respect to Si

Type	3 wt.% PHPS-derived SiO_x layer	5 wt.% PHPS-derived SiO_x layer
<i>(a) At.%</i>		
Si 2p	34.36	38.40
O 1s	63.36	56.44
N 1s	1.91	3.87
<i>(b) Atomic ratio</i>		
O/Si	1.84	1.47
N/Si	0.06	0.10

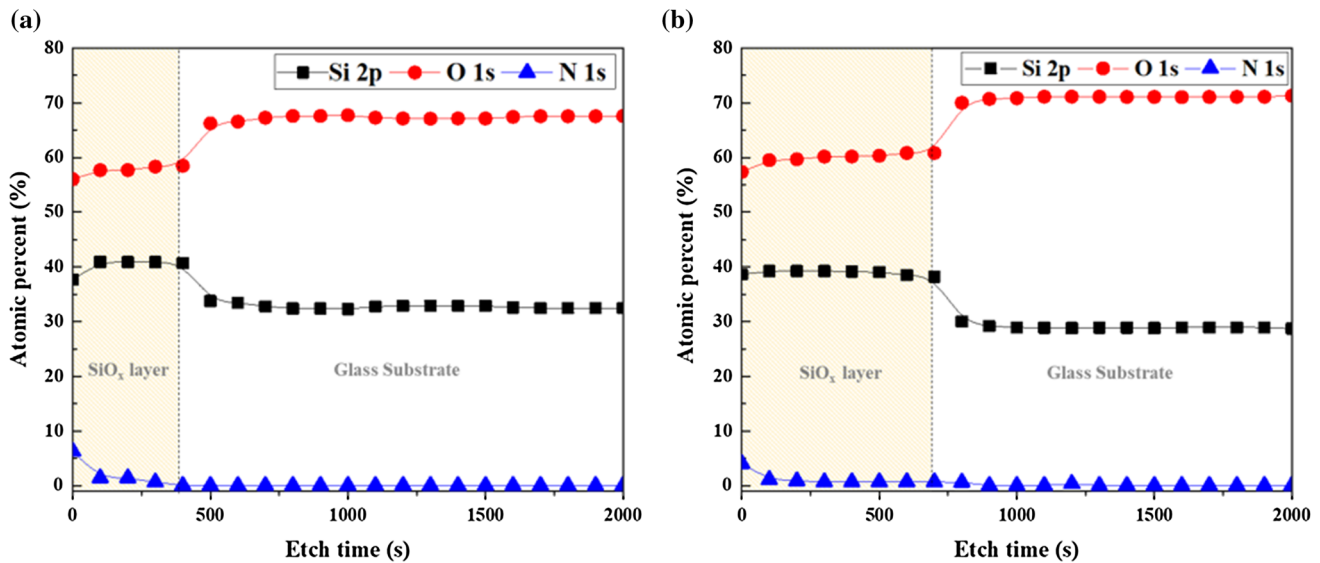


Figure 8 XPS depth profiles of the layers produced from **a** 3 wt.% and **b** 5 wt.% PHPS layers on glass substrates subjected to IPL irradiation at an applied energy of 12.6 J cm^{-2} .

Table 4 Surface properties of PET films, SiO_x layers derived from 3 and 5 wt.% PHPS on PET after IPL irradiation, and SiO_x layer derived from 5 wt.% PHPS on glass after heat treatment at $600 \text{ }^\circ\text{C}$

Sample	PET film	3 wt.% PHPS-derived SiO_x layer	5 wt.% PHPS-derived SiO_x layer	5 wt.% PHPS-derived SiO_x layer
Curing method	N.A	IPL irradiation (12.6 J cm^{-2})	IPL irradiation (12.6 J cm^{-2})	Heat treatment ($600 \text{ }^\circ\text{C}$)
Thickness (nm)	155,000	93 ± 1.7	160 ± 0.7	119 ± 0.7
Refractive index value	1.64	1.45	1.45	1.45
Water contact angle ($^\circ$) (Mean \pm STD)	74 ± 2	23 ± 2	32 ± 2	39 ± 3
Transmittance (%)	89.0	90.9	90.7	N.A
Roughness (R_a , nm) (RMS, nm)	8.614	0.289 (0.366)	0.330 (0.415)	0.583 (0.712)
		(12.049)		
Pencil hardness on PET (750 g)	H	4H	4H	N.A
Pencil hardness on Glass (1 kg)	N.A	9H	9H	9H

STD standard deviation, R_a average roughness, RMS root mean square, NA not applicable

curing processes of PHPS films, as reported previously [43].

The total transmittance values of the silica layers on the PET films derived from PHPS were over 90%, whereas the transmittance of PET was 89%, as shown in Fig. 9. This is owing to the change in the RI value of PHPS upon conversion to SiO_x (RI = 1.45), as reported by Mattsson [46]. The measured RI values of SiO_x layers derived from 3 or 5 wt.% PHPS solutions were identical at 1.45 (for comparison, the RI value of PET is 1.64), as shown in Table 4.

The pencil hardness of the PET film was measured as H at a load of 750 g, whereas the pencil hardness of the PHPS-derived SiO_x layer on the PET substrate prepared using 3 wt.% PHPS or 5 wt.% PHPS increased to 4H at a load of 750 g, as shown in Fig. 10 and Table 4. (Test method: KS M ISO 15184:2013). Moreover, the pencil hardness of the PHPS-derived SiO_x layer on the glass substrate and Si wafer prepared using the 3 wt.% or 5 wt.% PHPS solutions was 9H at a load of 1 kg.; In general, the thickness of coating layers, the stiffness of substrates and the difference in the conversion rate of SiO_x layer are

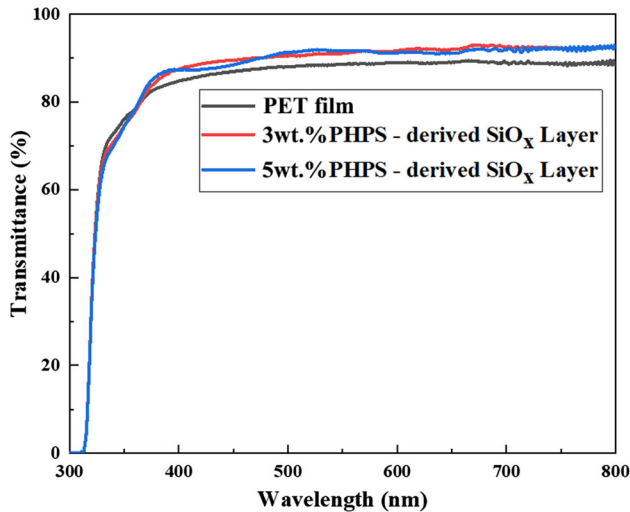
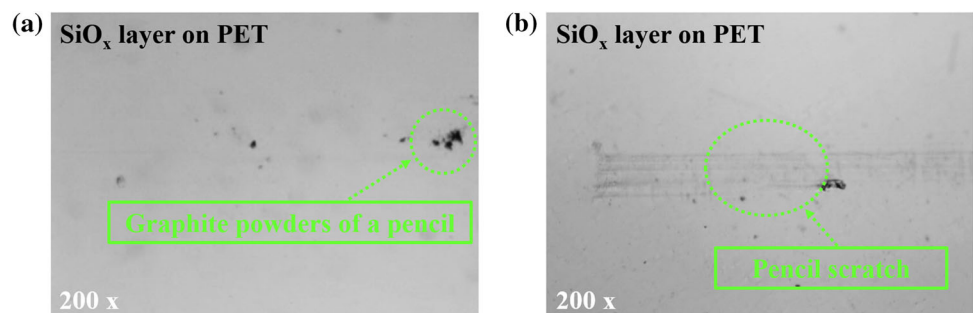


Figure 9 Transmittance spectra of 3 wt.% and 5 wt.% PHPS-derived SiO_x layers on PET films prepared using IPL irradiation at an applied energy of 12.6 J cm^{-2} .

contributed to hardness of coating layer. These results indicate that the effect of the PHPS concentration on pencil hardness in the thickness range of 93 nm to 160 nm was not significant. However, these pencil hardness results are higher than those for materials prepared using VUV irradiation, which was 6H at a load of 750 g when a Si wafer was used as a substrate [27]. Thus, the IPL process is much more effective at preparing PHPS-derived silica layers with better hydrophilicity, transparency, and hardness than conventional methods. Additionally, we evaluated the surface roughness of the materials using AFM to quantify flatness, and the results are shown in Fig. 11. The surface roughness was very low, with average roughness (R_a) values for materials prepared using 3 and 5 wt.% PHPS of 0.289 nm (RMS = 0.366) and 0.330 nm (RMS = 0.415), respectively, as shown in Table 4. These values indicate that the IPL-derived materials were much smoother than

Figure 10 Pencil hardness test images of 5 wt.% PHPS layers on PET substrate after IPL irradiation. Scratches made by a pencil at **a** 4H and **b** 5H under a load of 750 g.



PET, which has an R_a value of 8.614 nm (RMS = 12.049).

As shown in the FE-SEM surface images in Fig. 12a and b, the surfaces of the SiO_x layer materials were clear and uniform. Moreover, the cross-sectional images shown in Fig. 12c and d reveal a clear interface between the silica and the PET film, establishing a thin and dense silica layer with excellent adhesion to the PET film. For the additional cross-cut tape test results shown in Fig. 13 the grid was observed using an OM and 3D laser scanning confocal microscope, and the fraction of the meshes that underwent delamination was evaluated. No delamination was observed after removing the tape from the film. The 3 wt.% and 5 wt.% PHPS-derived SiO_x layers achieved the 5B classification for the standard ASTM D 3359 cross-cut test.

Thus, PHPS-derived SiO_x prepared using IPL processes is expected to be suitable for applications that require suitable hydrophilicity, transparency, flatness, adhesion, and hardness on flexible polymer films, such as in functional optical films (Table 4).

Nano-mechanical properties of SiO_x layers on PET film

Nano-indentation techniques are used to investigate the mechanical properties of inorganic layers. Hardness implies resistance to plastic deformation. The intrinsic hardness of thin films is evaluated at indentation depths ranging from 10 to 20% of the film thickness [47]. The nano-mechanical properties of the 3 and 5 wt.% PHPS-derived SiO_x layer materials were evaluated using nano-indentation at indentation depths that did not exceed 10% of the coating thickness. The measured load–displacement curves are shown in Fig. 14. Additionally, the elastic modulus and hardness were calculated by applying the Sneddon stiffness equation to analyze the load–

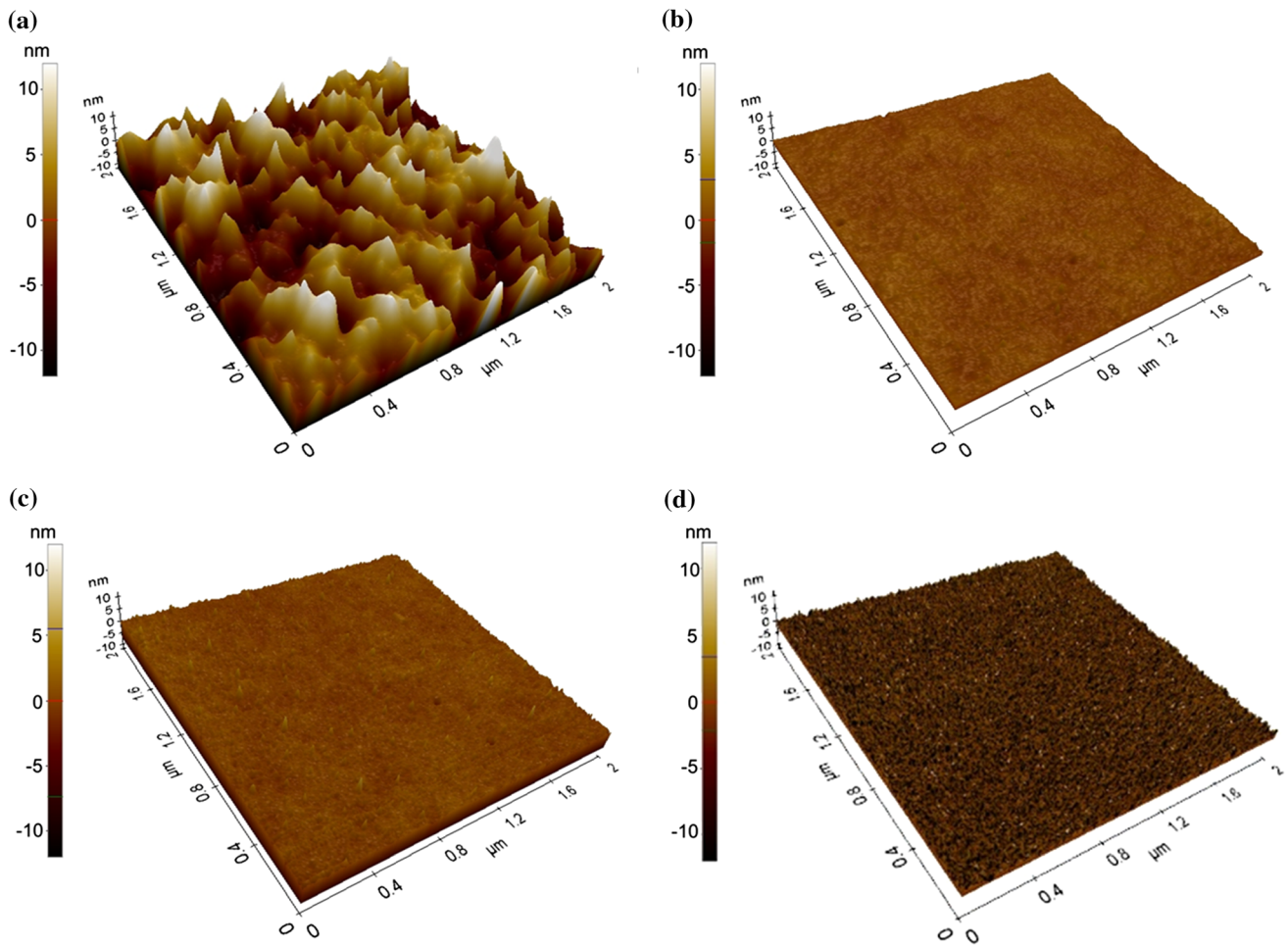


Figure 11 AFM images of **a** PET film, **b** 3 wt.%, and **c** 5 wt.% PHPS-derived SiO_x layers on PET films after IPL irradiation and **d** 5 wt.% PHPS-derived SiO_x layers on a PET film after 600 °C heat treatment.

Figure 12 Surface SEM images of **a** 3 wt.% and **b** 5 wt.% PHPS-derived SiO_x layers on PET films and cross-sectional SEM images of **c** 3 wt.% and **d** 5 wt.% PHPS-derived SiO_x layers on PET films.

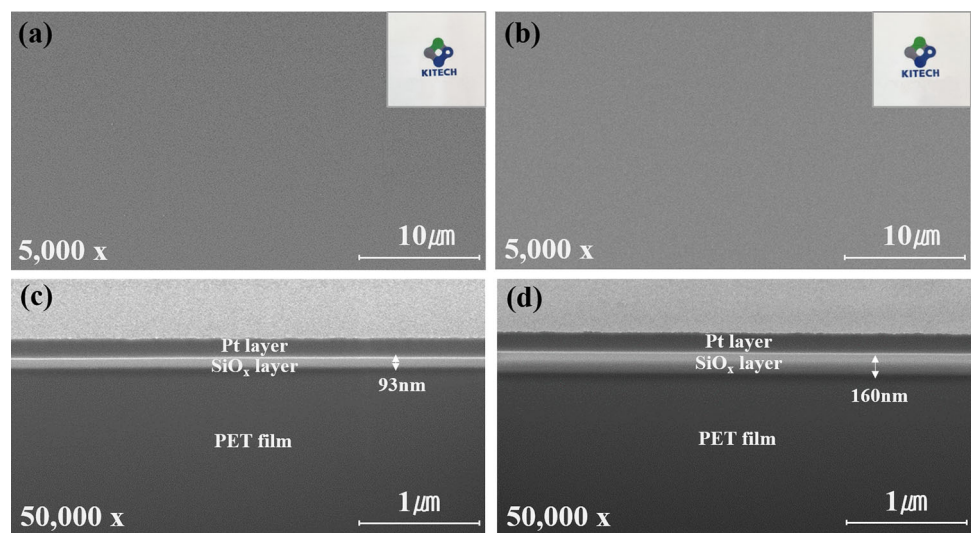


Figure 13 3D laser scanning confocal microscope images (left) and OM images (right) of SiO_x layers on PET substrate after cross-cut tape test to investigate the adhesion strength: **a** 3 wt.% PHPS-derived SiO_x layer and **b** 5 wt.% PHPS-derived SiO_x layer.

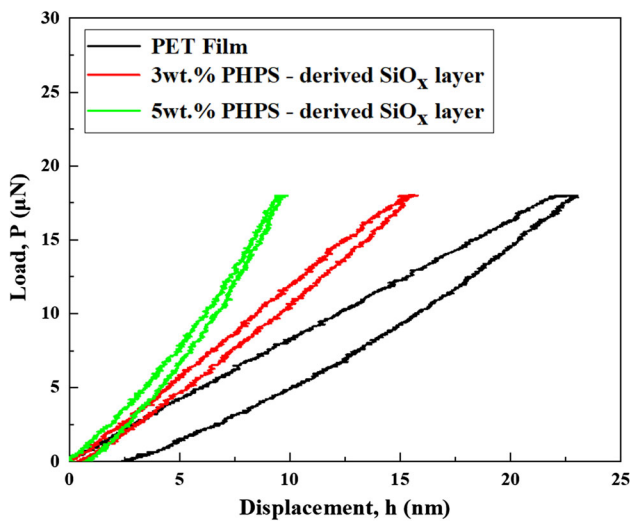
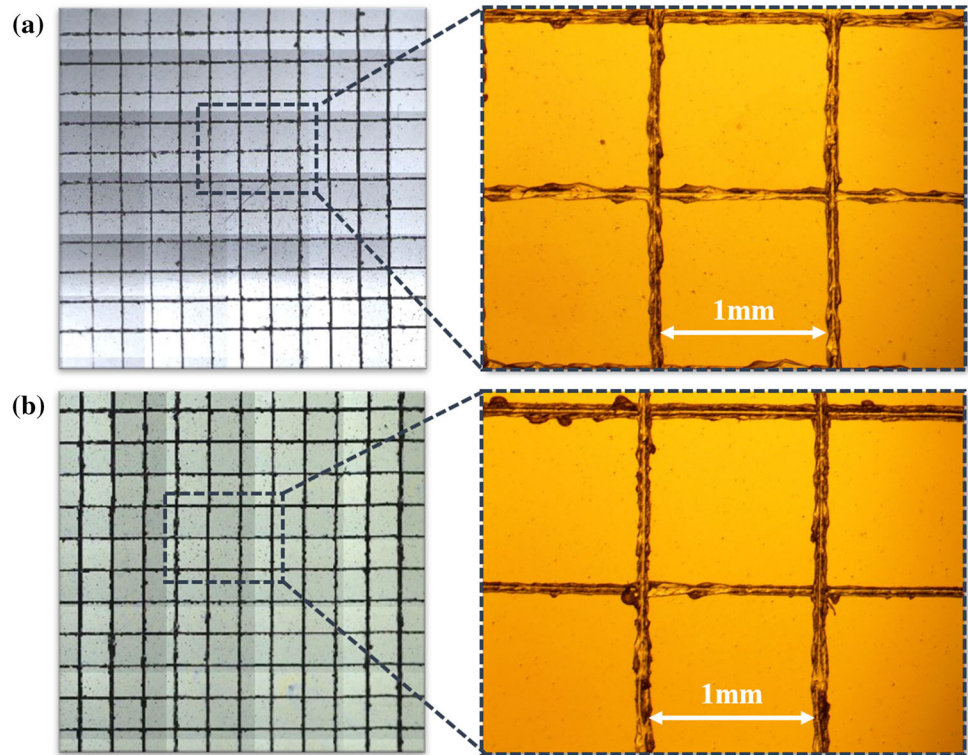


Figure 14 Load vs. displacement curves of films produced from 3 wt.% and 5 wt.% PHPS layers subjected to IPL irradiation obtained by using nano-indentation.

displacement curves acquired from each coating at five different positions. The Poisson’s ratio of the PET film and silica layers were 0.43 and 0.17, respectively.

As shown in Table 5, the mean hardness and elastic modulus of the 3 wt.% PHPS-derived SiO_x layer (thickness 93 ± 1.7 nm) were 2.61 GPa and 14.65 GPa, respectively. By comparison, the mean hardness

and elastic modulus of the 5 wt.% PHPS-derived SiO_x layers (thickness 160 ± 0.7 nm) were 3.25 GPa and 27.98 GPa, respectively. These values were similar to those for silica layers formed by roll-to-roll vacuum deposition coating in previous reports [47]. The hardness and elastic modulus were greater for the coated silica layer materials versus the bare PET film (1.15 GPa and 7.62 GPa, respectively). The hardness and elastic modulus also increased with increasing thickness of the silica layer, which was attributed to reduced elastic recovery because of the increased resistance to loads that originate from the higher silica content with increased thickness. Thus, the coating thickness should be reduced for roll-to-roll processing because the stiffness increases with increasing coating thickness.

Bending properties of SiO_x layers

A dynamic bending test was performed using a tension-free U-shape folding test machine to examine the flexibility and crack tendency of the 5 wt.% PHPS-derived SiO_x layers. The coated surface was folded inward and external compressive stress was applied to the coating surface. The bending tests were performed for 100,000 cycles at bending radii of 5, 3.5,

Table 5 Mechanical properties of PET films and SiO_x layers derived from 3 wt.% or 5 wt.% PHPS

Sample	PET film	3 wt.% PHPS-derived SiO _x layer	5 wt.% PHPS-derived SiO _x layer
Mean contact depth ± STD	11.97 ± 0.73	5.78 ± 0.42	4.96 ± 0.37
Mean hardness ± STD	1.15 ± 0.07	2.61 ± 0.26	3.25 ± 0.32
Mean elastic modulus ± STD	7.62 ± 0.86	14.65 ± 0.55	27.98 ± 0.84

STD standard deviation

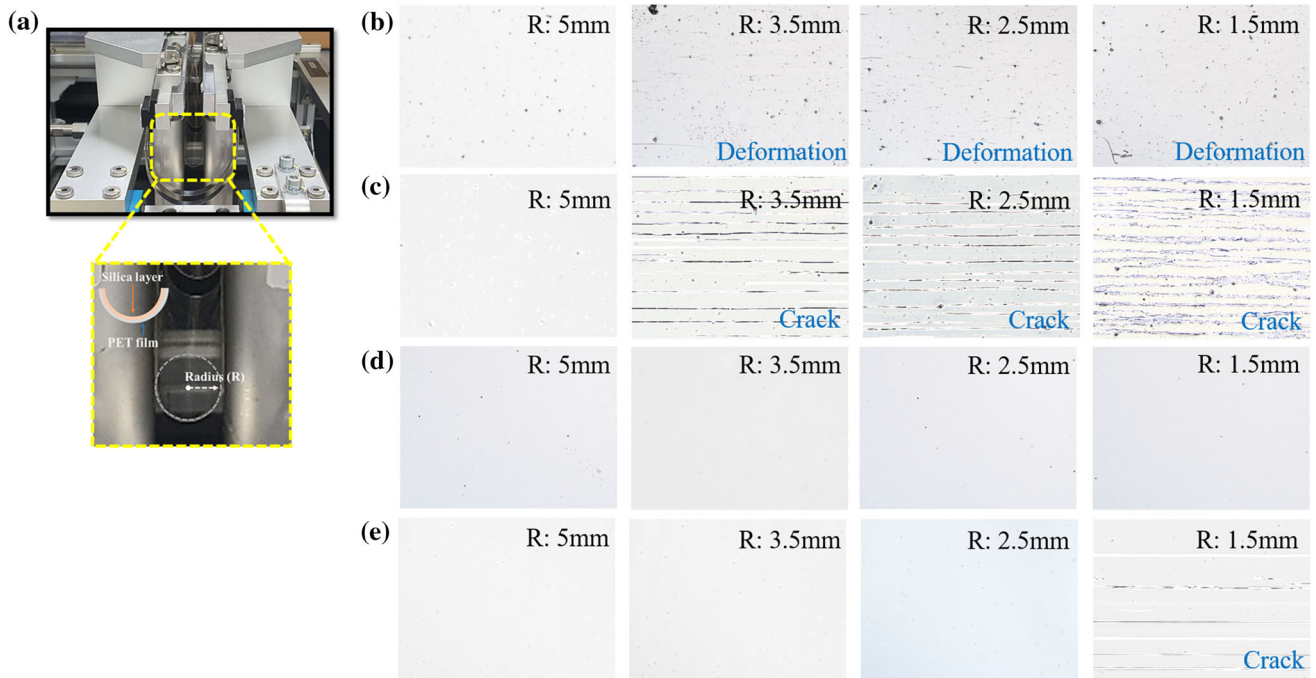


Figure 15 3D laser scanning confocal microscope images ($\times 96,000$) after bending test as a function of a radius over 100 K cycles: **a** dynamic folding test photograph of SiO_x, **b** bare

PET film, **c** 5 wt.% PHPS-derived SiO_x layer on PET film, **d** bare CPI film, and **e** 5 wt.% PHPS-derived SiO_x layer on CPI film.

2.5, 1.5 mm. After the bending test, the surfaces of the SiO_x layers were examined with the naked eye and a 3D laser scanning confocal microscope. As shown in Fig. 15, for a bending radius of 5 mm, no cracks or deformations were observed in any of the films. Under bending conditions of less than 3.5 mm, cracks and deformations were observed in the SiO_x layer on the PET film and a bare PET film (thickness 150 μm). In order to eliminate the influence of bare film, the bending tests using a CPI film (thickness 50 μm) were conducted. Notably, in the case of the 5 wt.% PHPS-derived SiO_x layer on CPI film, no cracks or deformations were observed after bending for 100,000 cycles at a radius of 2.5 mm. Because the bending property is vulnerable with increasing bare film thickness, film deformation occurs easily in

accordance with the equation for the bending stiffness of a film [48]. That is why the silica layer based on the thinner CPI film was not cracked at bending radii of 3.5 mm and 2.5 mm. These results demonstrate the feasibility of using PHPS-derived SiO_x layers as functional optical materials for flexible polymer films after IPL irradiation.

Conclusions

We investigated the chemical behavior, chemical composition, conversion rates, and final properties of silica layers produced by subjecting PHPS thin films to IPL irradiation at low temperatures in an air environment. This methodology serves as an

alternative to conventional processes such as heat treatment and vacuum deep ultraviolet treatment (VUV) for manufacturing functional optical films. The IPL processing technique converts the PHPS layer into a glass-like SiO_x layer. The resulting properties of the film varied with the total energy of the IPL irradiation, as confirmed by FT-IR spectroscopy, ellipsometry measurements, and XPS analyses. Moreover, the conversion rates of the Si–N and Si–H groups were estimated from the FT-IR absorption spectra, which enabled a comparison with silica layer materials prepared by heat treatment. IPL irradiation produced a silica layer (thickness 160 ± 0.7 nm) with a 100% conversion rate similar to that of a heat-treated silica layer (600 °C). This material also had a hydrophilic surface with an RI value of 1.45, identical to that of amorphous SiO_2 .

The IPL method can also be used to prepare functional silica films with thicknesses less than 160 nm on PET film substrates with excellent transmittance (> 90%), a pencil hardness of 4H at a load of 750 g (9H at a load of 1 kg on glass), good hydrophilicity (WCA of 23–32°), an adhesion strength of 5B, and low roughness ($R_a = 0.289\text{--}0.330$ nm and $\text{RMS} = 0.366\text{--}0.415$). Moreover, the mean hardness and mean elastic modulus of the IPL-derived SiO_x layer (thickness 93–160 nm) on PET film were 2.61–3.25 GPa and 14.65–27.98 GPa, respectively, values that are similar to those of SiO_x layers formed by roll-to-roll vacuum deposition. Furthermore, the IPL-derived silica layer exhibited no cracks for the bending test of 100,000 cycles with a radius of 5.0 mm (the layer on PET film) and 2.5 mm (the layer on CPI film). In conclusion, we established that the IPL process effectively converted PHPS into silica layers on flexible polymer films rapidly, in an air environment, and at low temperatures. Moreover, the IPL process did not require heat treatment or gas control equipment, as used for VUV. The IPL process can therefore be applied to roll-to-roll manufacturing in various electronic and functional optical film industries.

Acknowledgements

This study was conducted with the support of the Korea Institute of Industrial Technology under the grant entitled “Development of eco-friendly production system technology for total periodic resource cycle (KITECH EO-21-0014).”

Declarations

Conflict of interests The authors declare that they have no conflict of interest.

References

- [1] Tóvári E, Csontos M, Kriváchy T et al (2014) Characterization of $\text{SiO}_2/\text{SiN}_x$ gate insulators for graphene based nanoelectromechanical systems. *Appl Phys Lett* 105:18–22. <https://doi.org/10.1063/1.4896515>
- [2] Jacobson NS, Opila EJ, Lee KN (2001) Oxidation and corrosion of ceramics and ceramic matrix composites. *Curr Opin Solid State Mater Sci* 5:301–309. [https://doi.org/10.1016/S1359-0286\(01\)00009-2](https://doi.org/10.1016/S1359-0286(01)00009-2)
- [3] Roberts AP, Henry BM, Sutton AP et al (2002) Gas permeation in silicon-oxide/polymer (SiO_x/PET) barrier films: role of the oxide lattice, nano-defects and macro-defects. *J Memb Sci* 208:75–88. [https://doi.org/10.1016/S0376-7388\(02\)00178-3](https://doi.org/10.1016/S0376-7388(02)00178-3)
- [4] Noda T, Suzuki H, Araki H et al (1993) Microstructure and growth of SiC film by excimer laser chemical vapour deposition at low temperatures. *J Mater Sci* 28:2763–2768. <https://doi.org/10.1007/BF00356215>
- [5] Howells DG, Henry BM, Madocks J, Assender HE (2008) High quality plasma enhanced chemical vapour deposited silicon oxide gas barrier coatings on polyester films. *Thin Solid Films* 516:3081–3088. <https://doi.org/10.1016/j.tsf.2007.11.017>
- [6] Henry BM, Roberts AP, Grovenor CRM, et al (1998) Microstructural characterization of transparent silicon oxide permeation barrier coatings on PET. In: Proceedings, annual technical conference - society of vacuum coaters. pp 434–439
- [7] Leplan H, Robic JY, Pauleau Y (1996) Kinetics of residual stress evolution in evaporated silicon dioxide films exposed to room air. *J Appl Phys* 79:6926–6931. <https://doi.org/10.1063/1.361517>
- [8] Koutsonikolas DE, Kaldis SP, Pantoleontos GT (2017) Preparation of Silica Membranes by Atomic Layer Deposition. Elsevier B.V.

- [9] Kim J, Jang JH, Kim JH et al (2020) Inorganic encapsulation method using solution-processible polysilazane for flexible solar cells. *ACS Appl Energy Mater* 3:9257–9263. <https://doi.org/10.1021/acsaem.0c01593>
- [10] Morlier A, Cros S, Garandet JP, Alberola N (2013) Gas barrier properties of solution processed composite multilayer structures for organic solar cells encapsulation. *Sol Energy Mater Sol Cells* 115:93–99. <https://doi.org/10.1016/j.solmat.2013.03.033>
- [11] Morlier A, Cros S, Garandet JP, Alberola N (2014) Structural properties of ultraviolet cured polysilazane gas barrier layers on polymer substrates. *Thin Solid Films* 550:85–89. <https://doi.org/10.1016/j.tsf.2013.10.140>
- [12] Ohishi T (2003) Gas barrier characteristics of a polysilazane film formed on an ITO-coated PET substrate. *J Non Cryst Solids* 330:248–251. <https://doi.org/10.1016/j.jnoncrysol.2003.09.022>
- [13] Seul HJ, Kim HG, Park MY, Jeong JK (2016) A solution-processed silicon oxide gate dielectric prepared at a low temperature via ultraviolet irradiation for metal oxide transistors. *J Mater Chem C* 4:10486–10493. <https://doi.org/10.1039/c6tc03725a>
- [14] Kim SD, Ko PS, Park KS (2013) Perhydropolysilazane spin-on dielectrics for inter-layer-dielectric applications of sub-30 nm silicon technology. *Semicond Sci Technol* 28:1–6. <http://doi.org/10.1088/0268-1242/28/3/035008>
- [15] Urabe Y, Sameshima T (2008) Polysilazane precursor used for formation of oxidized insulator. *Mater Res Soc Symp Proc* 1066:107–111. <https://doi.org/10.1557/proc-1066-a05-02>
- [16] Bertocello R, Vezzoli A, Rebollo E (2016) Corrosion behaviour of room temperature cured polysilazane-derived silica coatings on Al 5086. *Int J Eng Res Science* 2:105–112
- [17] Günthner M, Kraus T, Krenkel W et al (2009) Particle-Filled PHPS silazane-based coatings on steel. *Int J Appl Ceram Technol* 6:373–380. <https://doi.org/10.1111/j.1744-7402.2008.02346.x>
- [18] Kozuka H, Nakajima K, Uchiyama H (2013) Superior properties of silica thin films prepared from perhydropolysilazane solutions at room temperature in comparison with conventional alkoxide-derived silica gel films. *ACS Appl Mater Interfaces* 5:8329–8336. <https://doi.org/10.1021/am400845y>
- [19] Isoda T, Kaya H, Nishii H et al (1992) Perhydropolysilazane precursors to silicon nitride ceramics. *J Inorg Organomet Polym* 2:151–160. <https://doi.org/10.1007/BF00696542>
- [20] Kamiya K, Oka A, Nasu H, Hashimoto T (2000) Comparative study of structure of silica gels from different sources. *J Sol-Gel Sci Technol* 19:495–499. <https://doi.org/10.1023/A:1008720118475>
- [21] Funayama O, Tahiro Y, Kamo A et al (1994) Conversion mechanism of perhydropolysilazane into silicon nitride-based ceramics. *J Mater Sci* 29:4883–4888. <https://doi.org/10.1007/BF00356538>
- [22] Kamiya K, Tange T, HASHIMOTO, H, NASU YS, (2001) Formation process of silica glass thin films from perhydropolysilazane. *ResRepFacEngMie Univ* 26:23–31
- [23] Kobayashi Y, Yokota H, Fuchita Y et al (2013) Characterization of gas barrier silica coatings prepared from perhydropolysilazane films by vacuum ultraviolet irradiation. *J Ceram Soc Japan* 121:215–218. <https://doi.org/10.2109/jcersj2.121.215>
- [24] Prager L, Dierdorf A, Liebe H et al (2007) Conversion of perhydropolysilazane into a SiO_x network triggered by vacuum ultraviolet irradiation: Access to flexible, transparent barrier coatings. *Chem a Eur J* 13:8522–8529. <https://doi.org/10.1002/chem.200700351>
- [25] Ohishi T, Yamazaki Y (2017) Formation and gas barrier characteristics of polysilazane-derived silica coatings formed by excimer light irradiation on PET films with vacuum evaporated silica coatings. *Mater Sci Appl* 8:1–14. <https://doi.org/10.4236/msa.2017.81001>
- [26] Ohishi T, Ichikawa K, Isono S (2020) Heat-resistant properties of a SiO₂-coated pet film prepared by irradiating a polysilazane-coated film with excimer light. *Mater Sci Appl* 11:58–69. <https://doi.org/10.4236/msa.2020.111005>
- [27] Naganuma Y, Horiuchi T, Kato C, Tanaka S (2013) Low-temperature synthesis of silica coating on a poly(ethylene terephthalate) film from perhydropolysilazane using vacuum ultraviolet light irradiation. *Surf Coatings Technol* 225:40–46. <https://doi.org/10.1016/j.surfcoat.2013.03.014>
- [28] Ohishi T, Yanagida K (2016) Preparation and gas barrier characteristics of polysilazane derived multi-layered silica thin films formed on alicyclic polyimide film using ultraviolet irradiation. *Front Nanosci Nanotechnol* 2:173–178. <https://doi.org/10.15761/FNN.1000131>
- [29] Ohishi T, Sone S, Yanagida K (2014) Preparation and gas barrier characteristics of polysilazane-derived silica thin films using ultraviolet irradiation. *Mater Sci Appl* 05:105–111. <https://doi.org/10.4236/msa.2014.53015>
- [30] Ohishi T, Yamazaki Y, Nabatame T (2016) Preparation, structure and gas barrier characteristics of polysilazane-derived silica thin film formed on PET by simultaneously applying ultraviolet-irradiation and heat-treatment. *Front Nanosci Nanotechnol* 2:149–154. <https://doi.org/10.15761/fnn.1000126>
- [31] Kubo T, Kozuka H (2006) Conversion of perhydropolysilazane-to-silica thin films by exposure to vapor from aqueous ammonia at room temperature. *J Ceram Soc Japan* 114:517–523. <https://doi.org/10.2109/jcersj.114.517>

- [32] Kozuka H, Fujita M, Tamoto S (2008) Polysilazane as the source of silica: the formation of dense silica coatings at room temperature and the new route to organic–inorganic hybrids. *J Sol-Gel Sci Technol* 48:148–155. <https://doi.org/10.1007/s10971-008-1793-1>
- [33] Kubo T (2004) Preparation of hot water-resistant silica thin films from polysilazane solution at room temperature. *J Sol-Gel Sci Technol* 31:257–261. <https://doi.org/10.1023/B:JSS T.0000047999.87439.c2>
- [34] Lee J, Oh J, Moon S et al (2010) A technique for converting perhydropolysilazane to SiO_x at low temperature. *Electrochem Solid-State Lett* 13:2009–2011. <https://doi.org/10.1149/1.3264092>
- [35] Druffel T, Dharmadasa R, Lavery BW, Ankireddy K (2018) Intense pulsed light processing for photovoltaic manufacturing. *Sol Energy Mater Sol Cells* 174:359–369. <https://doi.org/10.1016/j.solmat.2017.09.010>
- [36] Kang JS, Ryu J, Kim HS, Hahn HT (2011) Sintering of inkjet-printed silver nanoparticles at room temperature using intense pulsed light. *J Electron Mater* 40:2268. <https://doi.org/10.1007/s11664-011-1711-0>
- [37] Benwadih M, Coppard R, Bonrad K et al (2016) High mobility flexible amorphous IGZO thin-film transistors with a low thermal budget ultra-violet pulsed light process. *ACS Appl Mater Interfaces* 8:34513–34519. <https://doi.org/10.1021/acsami.6b09990>
- [38] Kim H-S, Dhage SR, Shim D-E, Hahn HT (2009) Intense pulsed light sintering of copper nanoink for printed electronics. *Appl Phys A* 97:791. <https://doi.org/10.1007/s00339-009-5360-6>
- [39] Back HS, Kim MJ, Baek JJ et al (2019) Intense-pulsed-UV-converted perhydropolysilazane gate dielectrics for organic field-effect transistors and logic gates. *RSC Adv* 9:3169–3175. <https://doi.org/10.1039/c8ra09831j>
- [40] Bauer F, Decker U, Dierdorf A et al (2005) Preparation of moisture curable polysilazane coatings: Part I. Elucidation of low temperature curing kinetics by FT-IR spectroscopy. *Prog Org Coatings* 53:183–190. <https://doi.org/10.1016/j.porgcoat.2005.02.006>
- [41] Zhang Z, Shao Z, Luo Y et al (2015) Hydrophobic, transparent and hard silicon oxynitride coating from perhydropolysilazane. *Polym Int* 64:971–978. <https://doi.org/10.1002/pi.4871>
- [42] Spectroscopy XP (2012) The conversion of perhydropolysilazane into sion films characterized by X-ray photoelectron spectroscopy. *J Am Ceram Soc* 95:3722–3725. <https://doi.org/10.1111/jace.12045>
- [43] Wang K, Gu M, Motz G et al (2013) Control of surface energy of silicon oxynitride films. *Langmuir* 29:2889–2896. <https://doi.org/10.1021/la304307y>
- [44] Oya K, Watanabe R, Sasaki S et al (2014) Surface characteristics of polyethylene terephthalate (PET) film exposed to active oxygen species generated via ultraviolet (UV) lights irradiation in high and low humidity conditions. *J Photopolym Sci Technol* 27:409–414. <https://doi.org/10.2494/photopolymer.27.409>
- [45] Nakajima K, Uchiyama H, Kitano T, Kozuka H (2013) Conversion of solution-derived perhydropolysilazane thin films into silica in basic humid atmosphere at room temperature. *J Am Ceram Soc* 96:2806–2816. <https://doi.org/10.1111/jace.12513>
- [46] Mat KE (1995) Plasma-enhanced growth, composition and refractive index of silicon oxy-nitride films. *J Appl Phys* 77:6616–6623. <https://doi.org/10.1063/1.359072>
- [47] Charitidis C, Logothetidis S (2005) Nanomechanical and nanotribological properties of carbon based films. *Thin Solid Films* 482:120–125. <https://doi.org/10.1016/j.tsf.2004.11.129>
- [48] Bae BS, Choi GM, Kim YH et al (2017) Flexible hard coating (Flex9h®) for foldable display cover plastic film. *Dig Tech Pap - SID Int Symp* 48:215–217. <https://doi.org/10.1002/sdtp.11665>

Publisher's Note Springer Nature remains neutral with regard to jurisdictional claims in published maps and institutional affiliations.